Marine Environmental Research 210 (2025) 107350

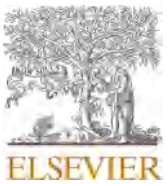

Contents lists available at ScienceDirect

Marine Environmental Research

journal homepage: www.elsevier.com/locate/marenvrev

The serious loss of mangrove forest over the largest delta of Africa, Niger Delta: causes and reasons

Diankai Wang [a], Zhijun Dai [a,b,*], Chuqi Long [c], Xixing Liang [a,d], Yuan Xiong [a], Jinping Cheng [c]

[a] State Key Laboratory of Estuarine and Coastal Research, East China Normal University, Shanghai, 200062, China
[b] Laboratory for Marine Geology, Qingdao Marine Science and Technology Center, Qingdao, China
[c] Department of Science and Environmental Studies, The Education University of Hong Kong, New Territories, Hong Kong, China
[d] Guangxi Key Laboratory of Marine Environmental Change and Disaster in Beibu Gulf, Beibu Gulf University (Qinzhou), 200062, China

ARTICLE INFO

Keywords:
Gain and loss
Mangrove forest
Oil spills
Niger delta
Machine learning technique

ABSTRACT

While global mangrove forests have suffered significant loss, raising widespread concern, little information is available on how mangrove forests have changed along Africa's coast. This study employed multi-temporal remote sensing data and machine learning techniques between 1988 and 2023 to assess the spatiotemporal changes in mangrove forests cover across the Niger Delta, Africa's largest delta. This results indicated a decreasing trend in mangrove area within the Niger Delta, with a total loss of 2536 km^2 over the past 38 years, leaving 7058 km^2 by 2023. The mangrove forests have become increasingly interiorly fragmented while retreating landward at an average rate of 13.58 m per year. Spatially, mangrove distribution remains concentrated in estuarine extensions, with most retreat occurring at mangrove edges. The intensification of oil spills and urban expansion likely contribute to the internal degradation within the Niger Delta's mangrove forests, of which 54.27 % of the mangrove loss may have been caused by oil spills. Meanwhile, high-energy waves are the primary driver of edge erosion, and variations in wave energy result in a gradual slowdown of the landward retreat of mangrove boundaries-from the central Arcuate Niger Delta toward its flanking regions. Furthermore, increased sediment discharge from river into coastal waters enhances mangrove expansion in estuarine zones, and accelerating sea-level rise presents a growing threat to mangrove sustainability. The findings provide critical insights into the drivers of mangrove gain and loss, offering actionable guidance for optimizing global mangrove conservation and restoration strategies.

1. Introduction

Mangrove forests are salt-tolerant plant communities, mainly distributed along tropical and subtropical coastlines, forming unique forest ecosystems (Hamilton, 2020; Tomlinson, 2016). They not only possess excellent primary productivity, providing indispensable habitats for a variety of species, but also make significant contributions to human societies by offering critical goods and services (Clough, 1992; Lee et al., 2014). Despite the undeniable importance of mangrove forests, they remain one of the most threatened ecosystems on the planet. Over the past fifty years, the global mangrove forest area has diminished by 30 %–50 % due to human activities (Food and Agriculture Organization of the United Nations, 2007). If this reduction trend continues, the ecosystem provided by mangrove forests could completely disappear within the next 100 years, causing irreversible damage to biodiversity and human societies (Duke et al., 2007).

Some studies indicated that mangrove forest ecosystems are currently facing unprecedented challenges from human activities (Eddy et al., 2021; Thomas et al., 2017). From 2000 to 2016, the total area of mangrove forests worldwide decreased by 3363 km^2 (Hagger et al., 2022). This loss is particularly significant in countries like Indonesia, Thailand, Vietnam, and Brazil. Indonesia, which has the largest reserves of mangrove forests globally, has experienced about a 30 % reduction due to human impact over the past decades (Arifanti et al., 2022). In Thailand's southern regions, extensive clearing of mangrove forests for shrimp farming has resulted in a loss of nearly 50 % of these critical habitats, severely impacting biodiversity (Thampanya et al., 2006). Vietnam has been founded a 38 % reduction in mangrove forest areas, largely due to the historical use of defoliants during the Vietnam War and subsequent conversion to aquaculture and coastal development

* Corresponding author. State Key Laboratory of Estuarine and Coastal Research, East China Normal University, Shanghai, 200062, China.
E-mail address: zjdai@sklec.ecnu.edu.cn (Z. Dai).

https://doi.org/10.1016/j.marenvres.2025.107350
Received 7 December 2024; Received in revised form 18 June 2025; Accepted 6 July 2025
Available online 11 July 2025

(Veettil et al., 2019). From 1990 to 2000, the Guangdong-Hong Kong--Macau Greater Bay Area saw a significant reduction in mangrove forest areas due to aquaculture and urban development. However, between 2000 and 2018, mangrove forest recovery in the region increased from 37.5 % of their 1990 levels to over 80 %, thanks to improved conservation efforts (Ling et al., 2024). This highlights the varying global efforts in mangrove forests conservation and restoration (Wang et al., 2021).

The survival and development of mangrove forests are also profoundly affected by their physical environment, particularly the dynamics of waves and tidal currents (Bryan et al., 2017; Cannon et al., 2020). Specifically, tidal currents can transport sediment resuspended by wave action and preferentially deposit it along the mangrove forest's seaward fringe (Furukawa and Wolanski, 1996; Vo Luong and Massel, 2006; Wolanski et al., 2006). Therefore, the elevation of the tidal flat at the mangrove edge can be raised, creating suitable environmental conditions for seedling establishment and facilitating the forest's seaward expansion (Alongi, 2009; Balke et al., 2011; Furukawa et al., 1997; Furukawa and Wolanski, 1996; MacKenzie et al., 2016; Woodroffe et al., 2016a,b). However, the efficacy of this process depends on the intensity and spatial pattern of the tidal currents (Horstman et al., 2015). Lovelock et al.'s (2015) research findings show that in a low-energy tidal currents environment, currents redistribute little sediment and therefore have only a minor effect on mangrove erosion and deposition. Moreover, when mangrove forest areas are frequently subjected to strong wave impacts, it can lead to severe erosion of tidal flats (Pilato, 2019; Sánchez-Núñez et al., 2019a,b), which leads to exposure of the roots and the landward retreat of mangrove forests (Alongi, 2009; Vo Luong and Massel, 2006). However, in high wave energy environments, large amounts of wave-driven marine sediments may accumulate on the coastline, forming barriers that avoid mangroves directly subjected to wave action (Hu et al., 2015; Sánchez-Núñez et al., 2019a,b; Van Santen et al., 2007). Thus, barriers can well prevent the mangroves from further retreat to the land (Long et al., 2021; Xiong et al., 2024). Therefore, the hydrodynamic characteristics influence the growth and distribution patterns of mangrove forests (Ball, 1988; Berger et al., 2008).

Meanwhile, the rise in sea levels caused by global warming presents a persistent risk of submersion for mangrove forests (Cazenave and Cozannet, 2014; Woodroffe et al., 2016b). This situation also leads to increased salinity in coastal soils, loss of sediments, and reduced stability of mangrove root systems, making them more susceptible to erosion and damage (Bennion et al., 2024; Carruthers et al., 2024; Dittmann et al., 2022). In addition to the impacts of the rise in sea levels, mangrove forests are highly susceptible to external forces, particularly under the sustained pressure of human disturbances and the severe impacts of global climate change, becoming increasingly fragmented (Hagger et al., 2022; Shirmohammadi et al., 2024). With the rapid advancement of urbanization and industrialization, substantial amounts of sewage and industrial wastewater are discharged into coastal and estuarine areas (Tuholske et al., 2021). The transportation of these wastewaters along coastlines, combined with oil spills, has led to a rapid decline in mangrove forest populations (Lotfinasabasl et al., 2013). Oil spills, in particular, result in long-term disappearance of mangrove forests, with significant impacts observed in Brazil, Australia, and the Bay of Bengal (Jaman, 2023; Lassalle et al., 2023). The effects of oil on mangrove forest ecosystems are predominantly negative, manifesting as physical smothering, chemical toxicity, and reduced biodiversity. For areas affected by oil pollution, effective restoration of mangrove forest habitats can be achieved through hydrological restoration and the planting of mixed-species seedlings (Santos et al., 2024).

Coastal urban expansion often involves land reclamation, transforming mangrove forests areas into useable land, which directly leads to the disappearance of mangrove forests (Tuholske et al., 2017; Wanzhen and Majid, 2024). The increase in industrial activities brought about by urban expansion results in the emission of a large amount of pollutants, including heavy metals, chemical waste, and domestic sewage. These pollutants enter mangrove forests areas, causing soil and water contamination and endangering the health of the mangrove forests (Shwetakshi, 2023; Wu et al., 2024). Furthermore, urban expansion leads to the fragmentation of mangrove forest habitats, decreasing the connectivity between mangrove forests and other natural ecosystems. This fragmentation results in reduced biodiversity and the degradation of ecological functions (Stiepani et al., 2021).

Against this global backdrop, some studies have focused on the dynamic changes of mangrove forests in the Niger Delta (Nababa et al., 2020a,b; Nwobi et al., 2020; O'Farrell et al., 2025). For example, James et al. (2007a,b)observed a notable landward retreat of the seaward mangrove edges, highlighting the loss of mangrove forests. Further, Nababa et al. (2020) used multi-epoch Landsat spectral-temporal metrics plus L-band SAR to generate high-accuracy land-cover maps for 1988, 2000 and 2013, then applied change-intensity and fragmentation metrics to quantify where the rate and extent of mangrove loss and degradation in the Niger Delta. Kuta et al. (2025) analysed Landsat-derived NDVI time series at spill versus control sites, statistically linking spill volume and exposure time to sustained declines in mangrove canopy health across the delta. O'Farrell et al. (2025) developed an AI workflow that combines Sentinel-1 SAR and machine learning to track oil-spill-driven mangrove die-off in Rivers State.

While earlier work in the Niger Delta has provided important maps of mangrove extent, comparatively few studies have paired those remote-sensing products with hydrodynamic processes and human activities together to explore the processes influencing mangrove dynamics (James et al., 2007a,b; Numbere, 2018). Therefore, the research on temporal and spatial changes of mangrove forests in the Niger Delta and their causes has been insufficient in comparisons with those of the world. With the improvement of supervised classification algorithm and the progress of remote sensing technology, this study adopts the integrated method of machine learning and remote sensing images. The aims of this study to (1) map dynamics of mangrove forests cover in the Niger Delta; (2) investigate the gain and loss in the mangrove forests; (3) identify the main driving factors influencing mangrove forests changes in the Niger Delta.

2. Materials and methods

2.1. Study area

The Niger Delta is a significant geographical and ecological region in western Africa, the largest delta of Africa, covering approximately 70,000 km^2 across several states including Ondo, Edo, Delta, Bayelsa, Rivers, Imo, Abia, Akwa Ibom, and Cross River (Izah, 2018) (Fig. 1A). The geographic profile of the region is arcuate with a convex outer edge facing the Atlantic Ocean, and 21 estuaries spread along its span (Sexton and Murday, 1994) (Fig. 6A). The Niger River flows into the northern part of the delta, bringing abundant freshwater resources to the area and forming a broad intertidal zone (Fig. 1B). Wave dynamics in the Niger Delta predominantly originate from the southwest, with wave heights generally ranging from 1.5 to 2 m (Dada et al., 2016). The area is influenced by semi-diurnal tides with a tidal range of 1.8 m, contributing to the complexity of tidal and wave dynamics (James et al., 2007b). Moreover, the delta is a globally significant oil-producing region, ranking as the sixth largest oil-producing country and the twentieth largest oil field in the world, with oil exploration having a significant impact on the local environment (Effiong and Ubi, 2012). Mangrove forests in the Niger Delta are mainly located in the intertidal zones behind beach ridges, covering an area of nearly 9000 km^2. Influenced by the riverine gentle slopes, the vegetation transitions from freshwater to salt-tolerant species, with saltwater intrusion from the river providing ideal growing conditions for halophytic plants (Abam, 1999). This has made the Niger Delta the fifth-largest mangrove forests region in the world, with its mangrove forests cover accounting for about 5 % of the global mangrove forests (I. I. Nababa et al., 2020). Generally, the Niger

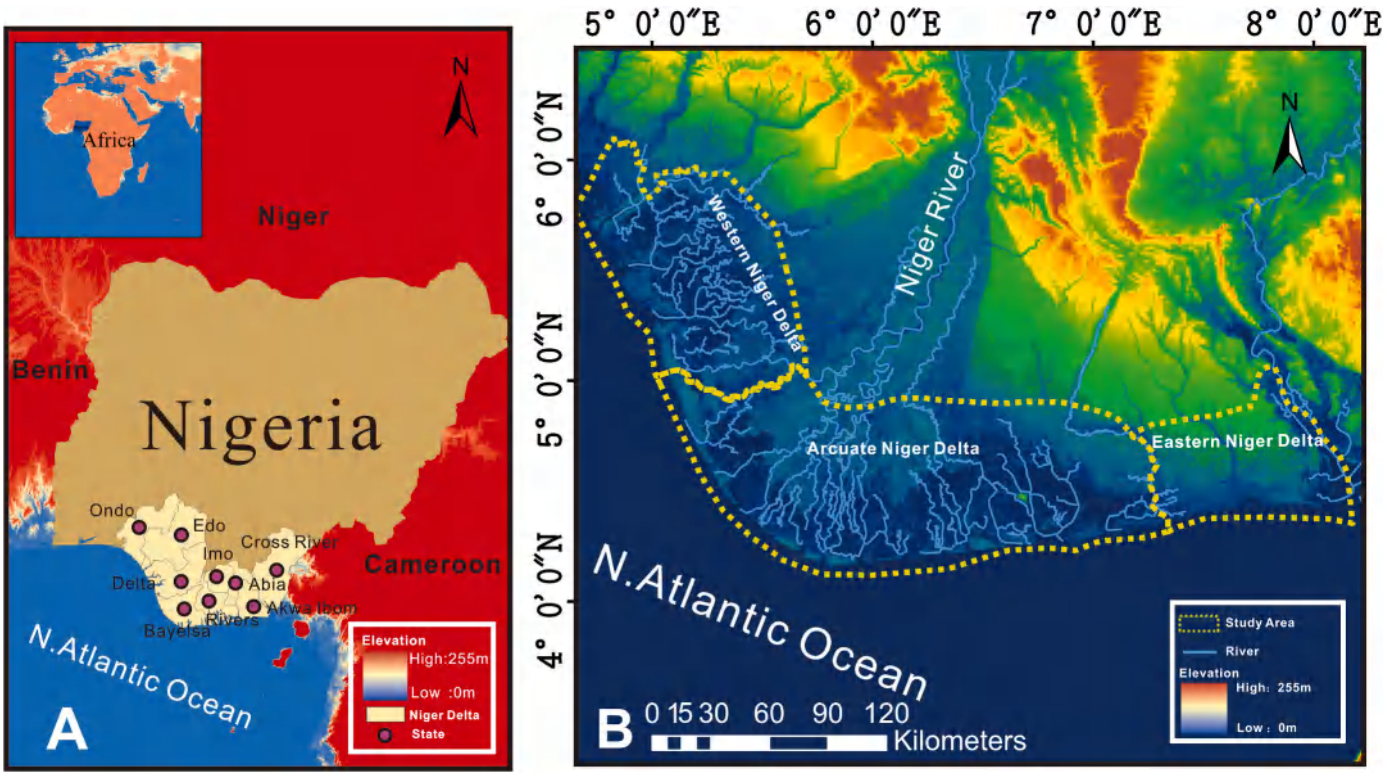

Fig. 1. Study area. (A) Location of the Niger Delta. (B) Detailed elevation map of the Niger Delta. (The base map originates from the Shuttle Radar Topography Mission's digital elevation data, https://www.gebco.net/).

Delta can be divided into three areas based on coastal distribution patterns: the Western Niger Delta, the Arcuate Niger Delta, and the Eastern Niger Delta (Dada et al., 2016) (Fig. 1B).

2.2. Materials

Using Google Earth Engine (GEE) (https://code.earthengine.google.com) from the image data, mainly from 1986 to 2023 all available cloud coverage less than 50 % of the time series Landsat images, it is classified by Random Forest algorithm and further adjusted in ArcGIS to ensure accuracy. The validation set combines data from Global Mangrove Watch Datasets (https://www.globalmangrovewatch.org/) with precise landmarks from Google Earth Pro, increasing the confidence of the data. The interannual spatial distribution map of mangrove forests was drawn. Landsat data sets include: LANDSAT/LT04/C01/T1_SR, LANDSAT/LT05/C01/T1_SR, LANDSAT/LE07/C01/T1_SR, LANDSAT/LC08/C01/T1_SR, and LANDSAT/LC08/C02/T1_L2. In the Niger Delta region of West Africa, there was a notable scarcity of early image data, particularly affecting the period from 1986 to 2012 (I. I. Nababa et al., 2020) (Fig. 2B). To address this, the study aggregated images over several years to facilitate geomorphic classification. Specifically, images from 1986 to 1988 were combined into a single composite scene. However, due to insufficient data from 1989 to 1998, it was difficult to create composites for this period. For subsequent years, composites were created for the periods 1999 to 2001, 2002 to 2006, 2007 to 2009, and 2010 to 2012. This approach enabled a relatively continuous and consistent analysis of geomorphological changes in the Niger Delta despite incomplete data.

Moreover, sea level data from 1993 to 2022, along with wave direction and wave height information for the study area, were obtained from the European Centre for Medium-Range Weather Forecasts (ECMWF) (https://cds.climate.copernicus.eu/cdsapp#!/home) (Figs. 11 and 7). Suspended sediment discharge was calculated from Landsat-derived suspended-sediment concentration products published by Dethier et al.

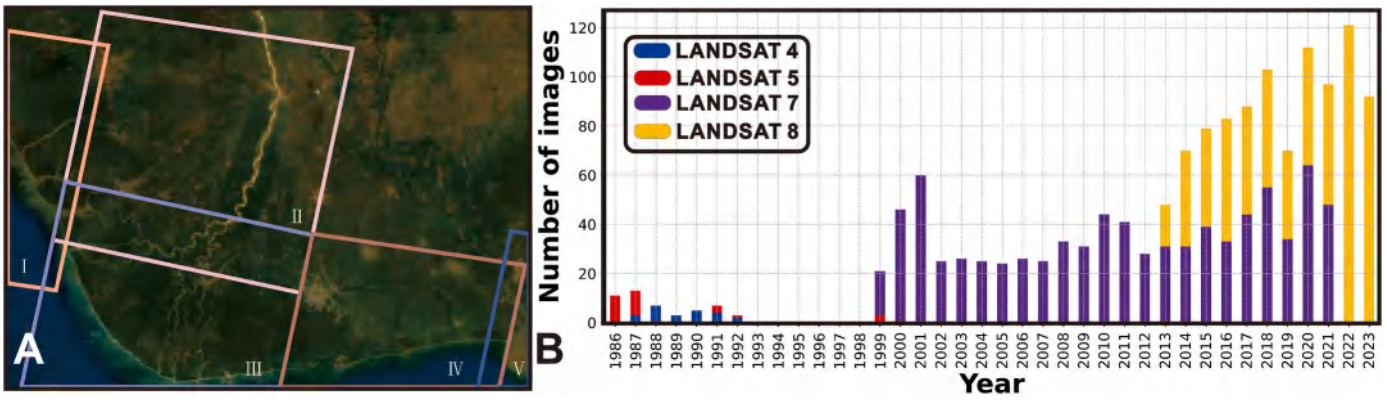

Fig. 2. Satellite imagery overview. (A) Satellite images location for delineating the bare beach edge. (B) The total number of satellite images.

(2022, 2020)(https://zenodo.org/records/7808492) (Fig. 6A). Oil Spills data were sourced from the Nigerian Oil Spill Monitor (https://oilspillmonitor.ng/) (Fig. 8).

2.3. Methods

2.3.1. Computation of spectral indices

Different landforms exhibit unique spectral characteristics, necessitating the identification of specific spectral properties (Montero et al., 2023; Williams et al., 2020). Surface reflectances across blue, green, red, near-infrared, and shortwave infrared bands were selected for analysis. Four spectral indices were calculated for each image on the GEE platform. These indices include the Normalized Difference Vegetation Index (NDVI) and the Enhanced Vegetation Index (EVI) (Ambrosini et al., 2014; Wardlow et al., 2007), which are critical for distinguishing vegetation from soil and water, enhancing the extraction of vegetation information and feature recognition. Additionally, the Modified Normalized Difference Water Index (NDWI) effectively identifies water bodies (Gao, 1996). The Mangrove Vegetation Index (MVI) is used to differentiate mangroves from non-mangrove vegetation and other non-vegetative covers such as bare soil, water, and buildings (Baloloy et al., 2020). These indices provide a robust framework for analyzing spectral data and understanding the geomorphological characteristics of the studied area. The formulas for calculating four spectral indices are as follows:

$$NDVI = \frac{\rho_{NIR} - \rho_{red}}{\rho_{NIR} + \rho_{red}} \quad (1)$$

$$EVI = 2.5 \frac{\rho_{NIR} - \rho_{red}}{\rho_{NIR} + 6\rho_{red} - 7.5\rho_{blue} + 1} \quad (2)$$

$$NDWI = \frac{\rho_{Green} - \rho_{NIR}}{\rho_{NIR} + \rho_{Green}} \quad (3)$$

$$MVI = \frac{\rho_{NIR} - \rho_{green}}{\rho_{SWIR1} - \rho_{green}} \quad (4)$$

where ρ_{NIR}, ρ_{red}, ρ_{blue}, ρ_{Green} and ρ_{SWIR1} represent the pixel values of the near-infrared, red, blue, green, and shortwave infrared one infrared bands of the Landsat images, respectively.

2.3.2. Machine learning method

Machine learning is now widely used in mangrove forests research (Deng et al., 2019; Fan et al., 2023; Ghosh et al., 2020; Hu et al., 2021; Pham and Brabyn, 2017; Wang et al., 2018; Xiong et al., 2024; Zhang et al., 2022). The Random Forest algorithm, a supervised machine learning method composed of multiple decision trees (Breiman, 2001), has been extensively applied in remote sensing, including biomass change detection and species identification (Sahana et al., 2022). Applying the random forest method to identify mangrove forests using the Google Earth Engine (GEE) platform is a method that integrates advanced remote sensing technology with a robust machine learning method to analyze and process large volumes of geospatial data (Fan et al., 2023; Jia et al., 2023; Wang et al., 2022; Xiao et al., 2024). In this context, the random forest method can examine multi-temporal, multi-band remote sensing image data acquired from GEE to accurately identify and monitor the distribution and changes in landforms (Teluguntla et al., 2018). In this scenario, the random forest method classifies the landforms into five categories: farmland, tidal flats, urban areas, water, and mangrove forests. Approximately 80 % of the samples are used for training (training set), while the remaining 20 % are used for validation (test set), this split is essential to assess the model's performance on new data and to prevent overfitting.

2.3.3. Digital Shoreline Analysis System (DSAS)

Digital Shoreline Analysis System (DSAS) is an ArcGIS plugin that provides automated methods for quantifying historical shoreline changes (Nassar et al., 2019). Within this framework, DSAS was utilized to calculate the variations in the edges of bare beach and mangrove forest edges across three regions at the same tidal level, thereby illustrating the lateral evolution of both environments under consistent tidal conditions. Specifically, the bare beach edge line at the same tidal level in 1986, 2001, 2006, 2011, 2016 and 2021 and the mangrove forests edge line in 1986, 2000, 2004, 2008, 2013, 2018 and 2023 were digitized, and the Linear Regression Rate (LRR) was calculated by DSAS to quantify the annual average edges change. The bare beach edges were depicted from five images selected based on consistent tidal levels predicted by tidal models (Table 1, Fig. 2A). Analyzing images based on the same tidal level effectively avoids inaccuracies in the results due to tidal coverage of the bare beach. The LRR calculates the slope of the least squares regression line that is fitted along the spline to all coastal points (Farris et al., 2023). This method is used to analyze the long-term changes of mangrove forests edges from 1986 to 2023, with a focus on minimizing short-term variations and potential random errors (Wang et al., 2014). Accordingly, a negative rate indicates erosion, where the coastline moves inland, and a positive rate suggests accretion, where the coastline advances seaward.

For comparing with sea level rise to determine the possible impacts of mangrove forests, the formula for calculating the average vertical sediment accumulation (AVSA) rate is as follows:

$$AVSA = V\tan\theta \quad (5)$$

where V is the average accretion rate of shorelines, and θ is the average slope in the Niger obtained from Dada et al. (2015), the average slope is 0.02 in Eastern Niger Delta and Western Niger Delta, and 0.05 in Arcuate Niger Delta.

2.4. Accuracy assessment

Machine learning outcomes are influenced by the resolution of remote sensing images and data processing methods, making error analysis essential for ensuring accurate research results (Heale and Twycross, 2015). For this purpose, we efficiently and accurately identified and classified mangrove forests in the target area using the Google Earth Engine (GEE) platform. In order to verify the accuracy of the classification results, we further used the survey data on Google Earth Pro (https://www.google.com/earth/about/versions/) and the Global Mangrove Watch (https://www.globalmangrovewatch.org/country/NGA) as the verification criteria, and used the confusion matrix to comprehensively evaluate the classification results (Comber et al., 2012). By calculating key performance metrics such as overall accuracy, user accuracy, producer accuracy, and the Kappa coefficient (Yao et al., 2022), which can ensure the high accuracy of the classification results.

3. Results

3.1. Variations in mangrove forest area

It can be found that from 1986 to 2023, the mangrove forests area in the Niger Delta presented a spiral decline, decreasing from an initial 9594 km^2 to 7058 km^2, a total loss of 2536 km^2, which represents 26.4

Table 1
Tidal levels of the images used to delineate bare beach edges.

Tide level (m)		Year					
		1986	2001	2006	2011	2016	2021
Image number	I	−0.75	−0.77	−0.75	−0.95	−0.92	−0.66
	II	−0.88	−0.72	−0.95	−0.72	−0.86	−0.88
	III	−0.84	−0.76	−0.99	−0.91	−0.93	−0.81
	IV	−0.43	−0.83	−0.98	−0.89	−0.87	−0.53
	V	−0.79	−0.79	−0.60	−0.91	−0.89	−0.71

% of the total mangrove forests area in 1986 (Fig. 3A). Specifically, from 1986 to 2000, mangrove forests coverage decreased by about 1380.7 km^2. It then increased by 267.8 km^2 from 2000 to 2004, but decreased by 346.7 km^2 from 2004 to 2008. Between 2008 and 2011, the area fell again by 209.7 km^2, then rose by 518.6 km^2 from 2011 to 2013, and by 66.3 km^2 from 2013 to 2014. The coverage dropped sharply by 705.6 km^2 from 2014 to 2015, but rebounded by 220.6 km^2 from 2015 to 2016, and by 345 km^2 from 2016 to 2017. It then fell by 503.2 km^2 from 2017 to 2018, rose by 481.4 km^2 from 2018 to 2019, dropped by 557.3 km^2 from 2019 to 2020, rose by 278.9 km^2 from 2020 to 2021, and finally decreased by 673.8 km^2 from 2021 to 2022 and by 337.4 km^2 from 2022 to 2023 (Fig. 3A).

Furtherly, there is an average loss of about 70.4 km^2/yr between 1986 and 2023, reflecting the rapid degradation of the mangrove forest ecosystem (Fig. 3A). Meanwhile, the variation patterns vary across different areas (Fig. 3B, C, and 3D). Between 1986 and 2023, in the Eastern Niger Delta, mangrove forests area decreased from an initial 529 km^2–218 km^2 (Fig. 3B), the Arcuate Niger Delta was founded a reduction from 5973 km^2 to about 4597 km^2 (Fig. 3C), and the Western Niger Delta decreased from 3091 km^2 to approximately 2244 km^2 (Fig. 3D). Clearly, the Eastern Niger Delta experienced the fastest rate of decrease, followed by the Arcuate Niger Delta, with the Western Niger Delta showing a relatively slower rate.

3.2. Changes in mangrove forest edges

Mangrove forest edges have retreated by 489.06 m from 1986 to 2023, while the bare beach edges have advanced by 6.12 m of the observed period (Fig. 4). Specifically, in the Western Niger Delta, mangrove forest edges have retreated by 198.36 m, while the bare beach edge has advanced by 81.72 m. However, in the Arcuate Niger Delta, mangrove forest edges and bare beach edges presented landward recession of about 717.06 m and 0.25 m, respectively. Similarly, in the Eastern Niger Delta, mangrove forest edges retreated 182.40 m and the bare beach edges retreated 8.28 m, respectively (Fig. 4A and B). From the erosion and accretion percentage of the bare beach edges samples, the accretion percentage decreased gradually from the Western Niger Delta to the Eastern Niger Delta, from 60.1 % to 41.9 % (Fig. 4D). In terms of erosion and accretion percentage of mangrove forest line samples, the number of erosion samples was greater than the number of accretion samples, which also showed that the accretion percentage decreased gradually from the Western Niger Delta to the Eastern Niger Delta, from 38.3 % to 19.5 % (Fig. 4C).

3.3. Gain and loss of the mangrove forest area

Over the past 38 years, the total area of mangrove forest across three regions has decreased by 3282.8 km^2. The Arcuate Niger Delta experienced the most severe reduction, losing 1727.7 km^2 of mangrove forest cover (Fig. 5G). Although the overall trend indicates a decrease in mangrove forest coverage, there was also a concurrent increase of 746.9 km^2 in the mangrove forest area of the Niger Delta during the same period (Fig. 5H), mainly gain in the estuary area and the Western Niger Delta, partially offsetting the overall loss. The change in mangrove forest area shows clear cyclical fluctuations, from 1986 to 2023, there was a pattern of loss and gain, specifically. From 1986 to 2000, despite an increase of 754 km^2 in mangrove area, the net loss was 1380.8 km^2, resulting in a net decline of 626.8 km^2 across all three regions, with significant retreats along the mangrove forest edges (Fig. 5A). From 2000 to 2004, particularly in the Western Niger Delta and the Arcuate Niger Delta, there was a recovery of mangrove forest, notably in the western of Arcuate Niger Delta (Fig. 5B). Between 2004 and 2008, the

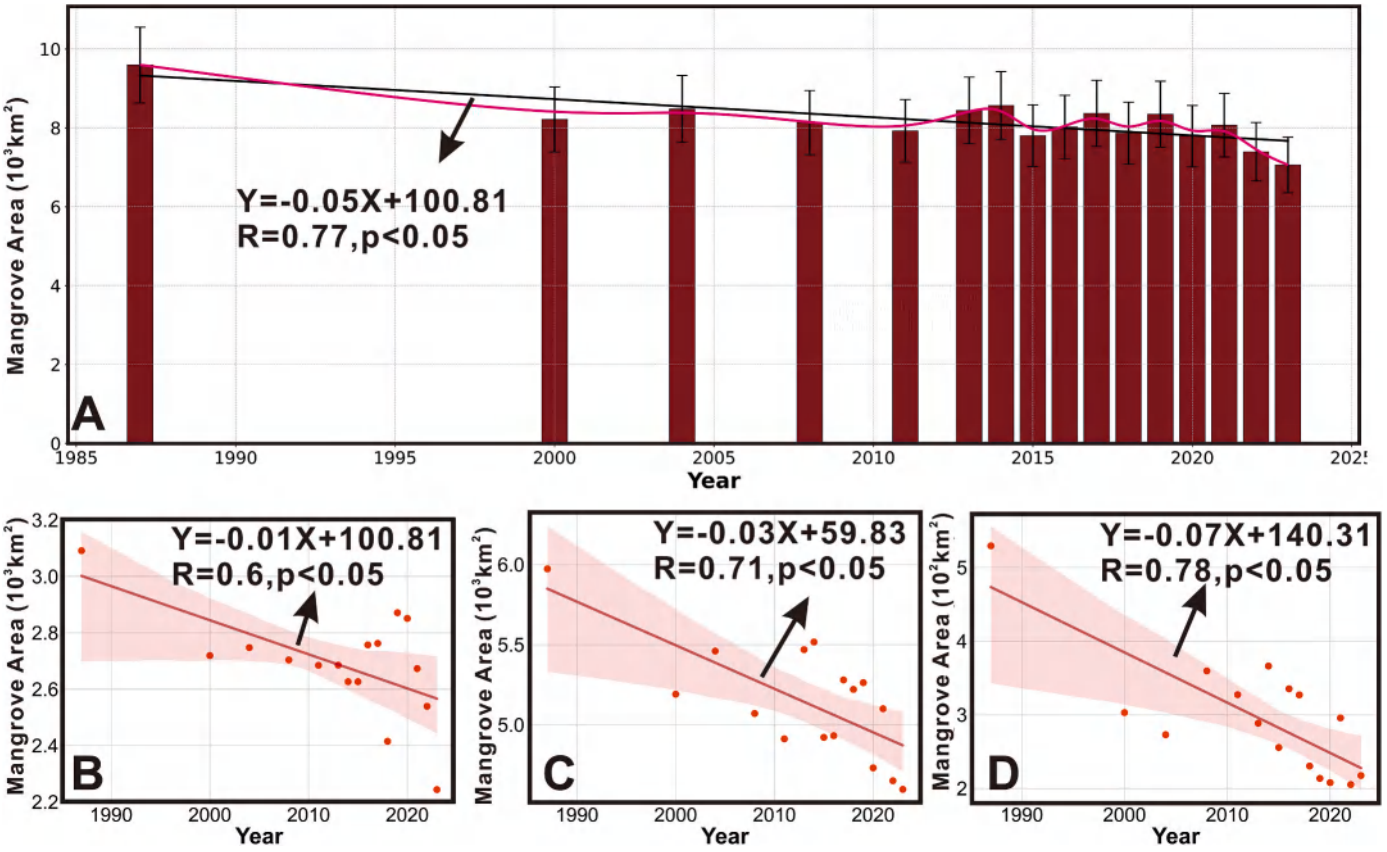

Fig. 3. Temporal variation of mangrove forests area in the Niger Delta. (A) Temporal variation of total mangrove forests area and spirals down (B) Western Niger Delta. (C) Arcuate Niger Delta. (D) Eastern Niger Delta.

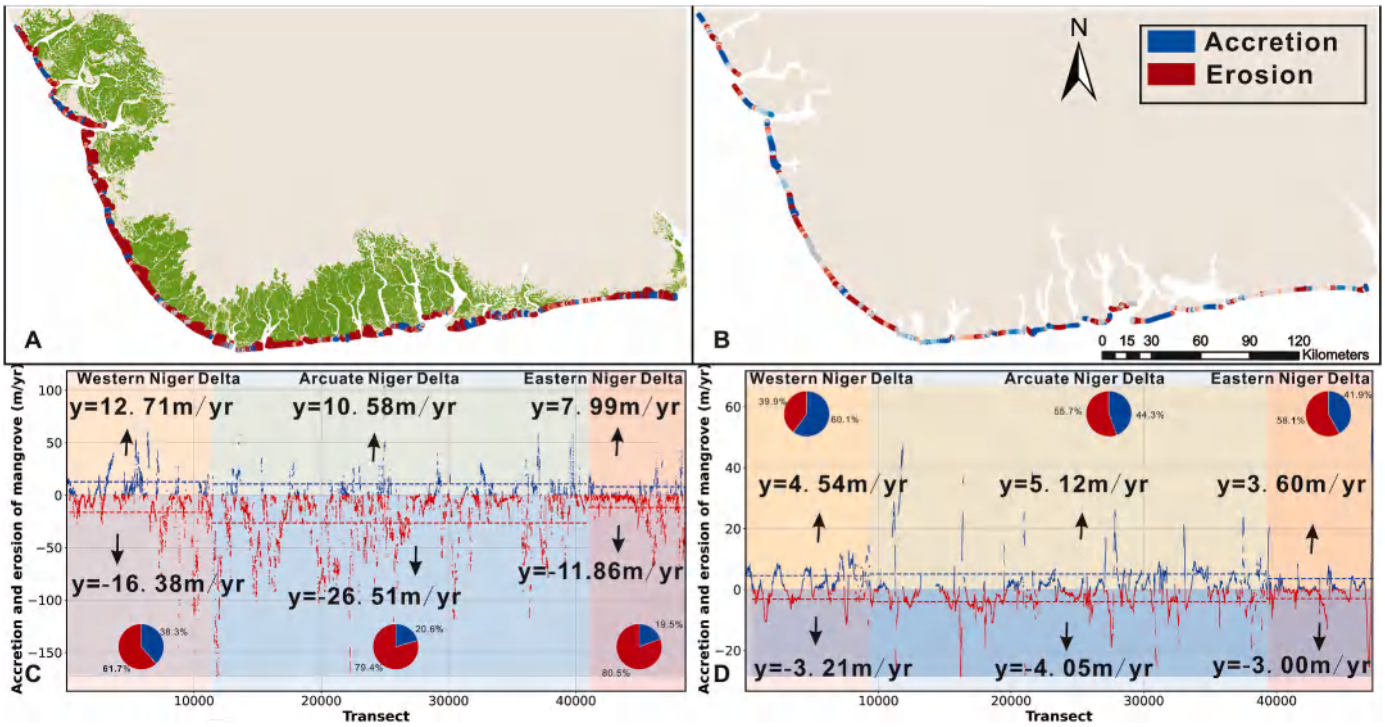

Fig. 4. Accretion and erosion of bare beach edges (1986–2021) and mangrove forest edges (1986–2023) in the Niger Delta. (A) Accretion and erosion of mangrove forest edges. (B) Accretion and erosion of bare beach edges. (C) LRR analysis for mangrove forest edges, with orange representing the mean values. (D) LRR analysis for bare beach edges, with orange indicating the mean values. In (C) and (D), pie charts represent accretion and erosion numbers as a percentage of the respective regional sample. (For interpretation of the references to colour in this figure legend, the reader is referred to the Web version of this article.)

mangrove forest area in the Eastern Niger Delta significantly increased, however, the overall trend during this period continued to be a decline (Fig. 5C). Between 2008 and 2013, mangrove forest recovered in the Arcuate Niger Delta and Western Niger Delta (Fig. 5D). From 2013 to 2018, the Arcuate Niger Delta exhibited a trend of alternating loss (Fig. 5E). Finally, from 2018 to 2023, despite severe loss in the Arcuate Niger Delta and Western Niger Delta (Fig. 5F). In summary, a comprehensive analysis of the gain and loss of mangrove forest reveals the spatial distribution of mangrove forest showed landward retreat and intensified fragmentation (Fig. 5G).

4. Discussion

4.1. Impacts of the suspended sediment discharge from upstream

The increased upstream Suspended Sediment Discharge (SSD) has complex implications for coastal accretion and the mangrove forest ecosystem (Liu et al., 2023). As one of the largest sedimentary environments globally, the Niger Delta's arc-shaped coastline is primarily maintained by an abundant input of sediments (George et al., 2019). Between 1986 and 2020, SSD from upstream surged from 1366.6 million tons/yr to 3446.9 million tons/yr, a 2.5-fold increase (Fig. 6B). The significant rise in river sedimentation is primarily concentrated in the Western Niger Delta and Arcuate Niger Delta, where 21 estuaries converge (Dada et al., 2018) (Fig. 6A). Consequently, these areas exhibited a trend of mangrove forest seaward accretion over 38 years (Fig. 4A), with the mangrove forest edges in the Western Niger Delta advancing by 483.0 m, in the Arcuate Niger Delta by 402.0 m, and in the Eastern Niger Delta by 303.6 m over the same period, the trend of mangrove forest spreading to the sea in the Western Niger Delta is obviously higher than that in the Eastern Niger Delta and Arcuate Niger Delta (Fig. 4A and B). Furtherly, these seaward expanded area were mainly located in those of the estuarine locations in Western Niger Delta and Arcuate Niger Delta, which can obtain enough sediment amounts from upstream (Fig. 5), while coastal zone without riverine sediment supplied presented erosion (Fig. 4A and B). In summary, the expansion of mangrove forest over the Niger delta can be partially attributed to the increased SSD from upstream.

4.2. Impacts of wave and tidal forcings

The Niger Delta, located in an environment free of cyclones and storms, is predominantly influenced by tidal currents and waves (Almar et al., 2015). The region experiences consistently high wave energy, with an average significant wave height of 1.36 m and a period of 9.6 s (Dada et al., 2018). The wave intensity in the Niger Delta increases from Western to Eastern Niger Delta and then decreases, with the greatest impact observed in the Arcuate Niger Delta, followed by the Eastern Niger Delta and Western Niger Delta (Fig. 7C–E). To better understand the relationship between wave action and mangrove forest edges erosion, a correlation analysis was conducted using mangrove erosion or expansion rate data of 10 sections covering the eastern and western deltas, analyzing the relationship between average wave height and mangrove forest erosion in these areas, revealing obvious correlation between the two, the significance level was below 0.05 (Fig. 7F), suggesting that wave action likely controls the retreat of the mangrove forest edges. It is important to note that the wave in Arcuate Niger Delta is strong and has a higher impact on coastal erosion than the Eastern Niger Delta, but the Niger River's sediment in Arcuate Niger Delta replenishment alleviates the wave's coastal erosion to a certain extent, which is why the percentage of mangrove forest edges retreat is increasing from Western Niger Delta to Eastern Niger Delta (Fig. 4C). Consequently, variations in wave intensity lead to varying degrees of mangrove forest retreat: the stronger the waves, the more severe the retreat.

Meanwhile, tidal currents exhibit an increasing trend from Western Niger Delta to Eastern Niger Delta, with nearshore currents showing a dispersal pattern from the Arcuate Niger Delta towards both the Eastern

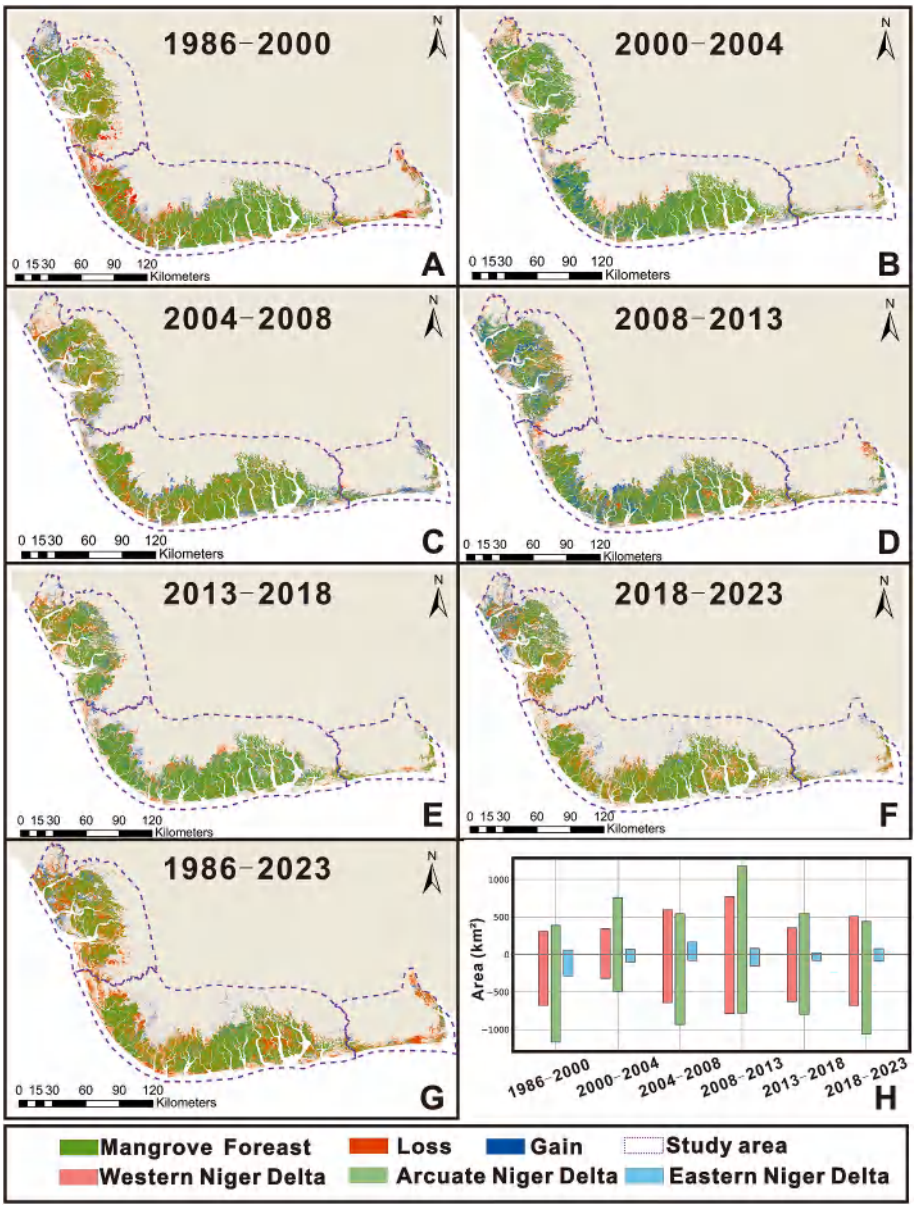

Fig. 5. Gain and loss of mangrove forest area in the Niger Delta. (A–G) Spatial distribution of mangrove forests during 1986–2023. (H) loss and gain areas of the seven periods.

Niger Delta and Western Niger Delta; in offshore areas, the flow of currents is predominantly from Western Niger Delta to Eastern Niger Delta (Fig. 7B). The tidal range in the region increases from 1.4 m in the Western Niger Delta to 2.0 m in the Eastern Niger Delta, indicating total weak tidal influences in the Western Niger Delta compared to the Eastern Niger Delta (Stutz and Pilkey, 2002). In briefly, the regional weak tidal range and the dispersal pattern of tidal current had no significant effect on the erosion and deposition of mangrove forest along the Niger River Delta coast, although tidal currents can also lift mangrove growth by carring sediment transport into the deposit of 900, 000 tons/yr of tidal sediment provides important living space for mangroves, thus easing the erosion of mangrove edges (Dada et al., 2018).

Additionally, barrier islands are extensively developed in Niger Delta, stretching for more than 300 km along the coast. These barriers average 16 km in length and 3.3 km in width, formed by high-energy wave conditions and tides (George et al., 2019; Stutz and Pilkey, 2002) (Fig. 7A). The presence of estuarine beach ridges and barriers plays a some role in protecting mangrove forest from the impacts of strong waves and tidal energies, providing a favorable environment for their growth (Long et al., 2021), and shielding the interior mangroves on barrier islands from wave erosion (Fig. 7A).

4.3. *Impacts of anthropogenic activities*

Human activities significantly impact mangrove forest loss (Chang et al., 2022; Chen et al., 2020), with oil pollution posing a severe threat to mangrove ecosystems (Lassalle et al., 2023; Onyena and Sam, 2020). The Niger Delta, which possesses Africa's largest oil reserves (Linden and Palsson, 2013), frequently suffers oil spills due to outdated extraction techniques and oil theft (Iwegbue et al., 2021) (Fig. 9A–C). Data indicate that from 2006 to 2023, a total of 8,546,250 barrels of oil were spilled, primarily in the Arcuate Niger Delta and Western Niger Delta mangrove forest regions (Fig. 8A–D). Notably, a single spill event can result in the loss of 836 ha of mangrove forest (Raji and Abejide, 2013). Mangrove forests, sensitive to oil pollution, have suffered extensive damage, leading to a decrease in cover in affected areas (Fig. 8E). The impact of oil spills on mangrove forest ecosystems is multifaceted. First, oil spills are not merely one-off events; their effects on ecosystems are

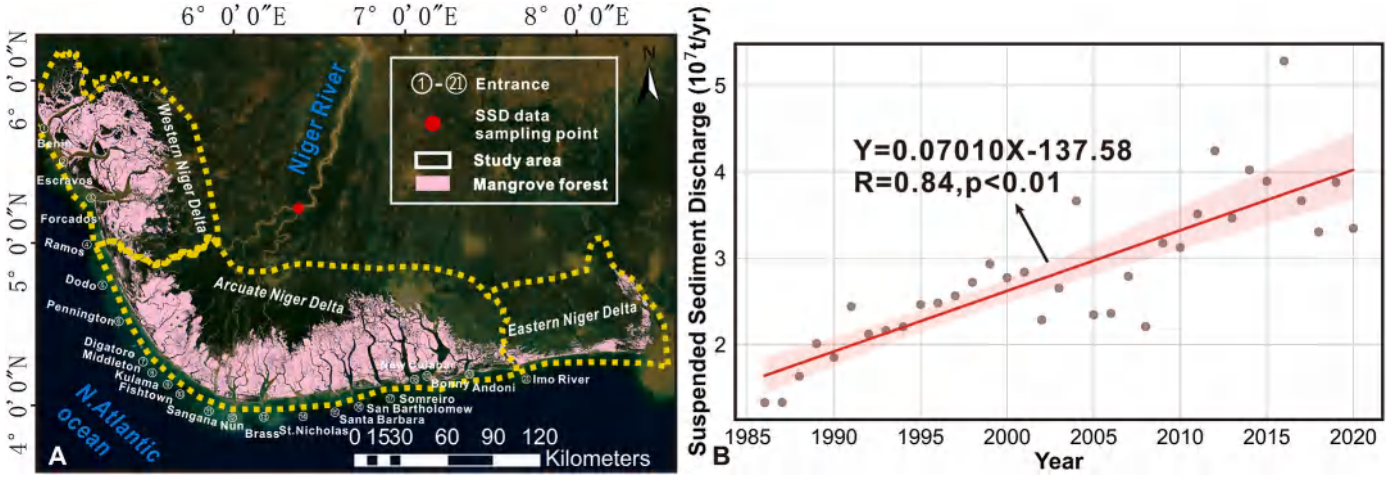

Fig. 6. The location where upstream SSD feeds into the Atlantic Ocean. (A) SSD data sampling location and 21 estuaries. (B) Temporal trends in SSD from 1985 to 2020. (https://zenodo.org/records/7808492).

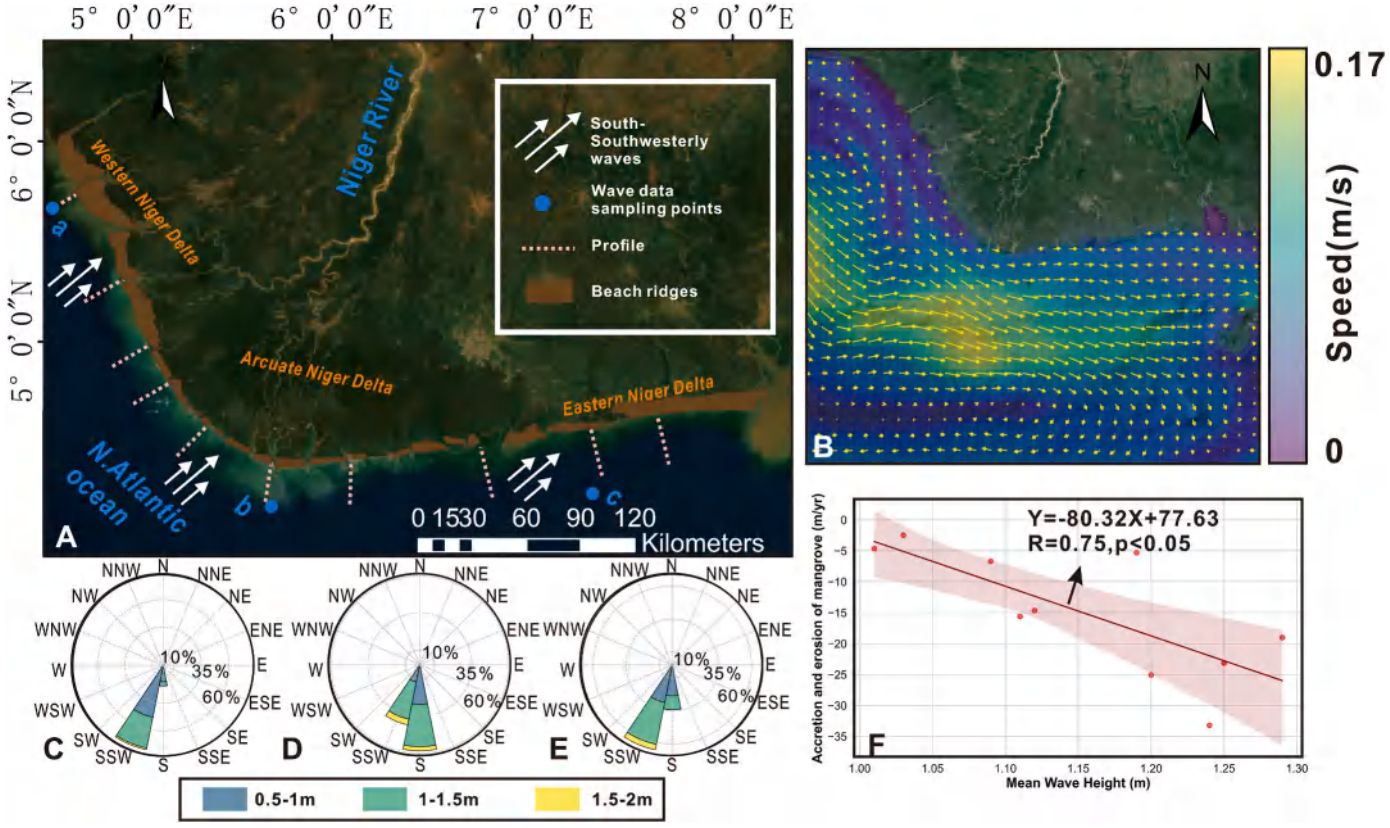

Fig. 7. The characteristics of wave and tidal forcings. (A) Wave current directions and beach ridge positions across the Western, Arcuate, and Eastern Niger Delta, with indicated wave data sampling points and erosion profiles. (B) Visualization of tidal current speeds. (C, D, E) Wave characteristics at locations a, b, and c. (F) Correlation between sediment yield rate and average wave height, showing a negative relationship.

long-term and persistent (Saunders et al., 2022). Oil spills can suffocate mangrove forest pneumatophores and root systems, alter soil properties, release toxic heavy metals, degrade ecosystems, and reduce biodiversity (Essien and Antai, 2009; John and Okpokwasili, 2012; Nwankwo, 2000; Onyena and Sam, 2020) (Fig. 9D–F). Up to now, mangrove forest loss due to oil spills increased from 13.3 % (2006–2008) to 45.28 % (2018–2023), Overall, oil spills accounted for 54.27 % of mangrove forest loss during this period (Fig. 8F), indicating that oil spills have become one of the primary drivers of mangrove forests decline in the Niger Delta, this also means that the mangrove forests in the whole region are still decreasing due to the oil spills (Fig. 8E).

Moreover, urban expansion poses a significant threat to mangrove forests. The acceleration of urbanization is typically accompanied by infrastructure development, land reclamation, and population growth, directly encroaching on mangrove habitats and causing their area to decline sharply (Moschetto et al., 2021). Urban expansion not only occupies significant mangrove areas but also exacerbates ecological degradation by altering hydrological conditions, increasing pollutant discharge, and disrupting habitats (Mosquera et al., 2023) (Fig. 10A and B). Correlation analysis shows that a significant negative correlation

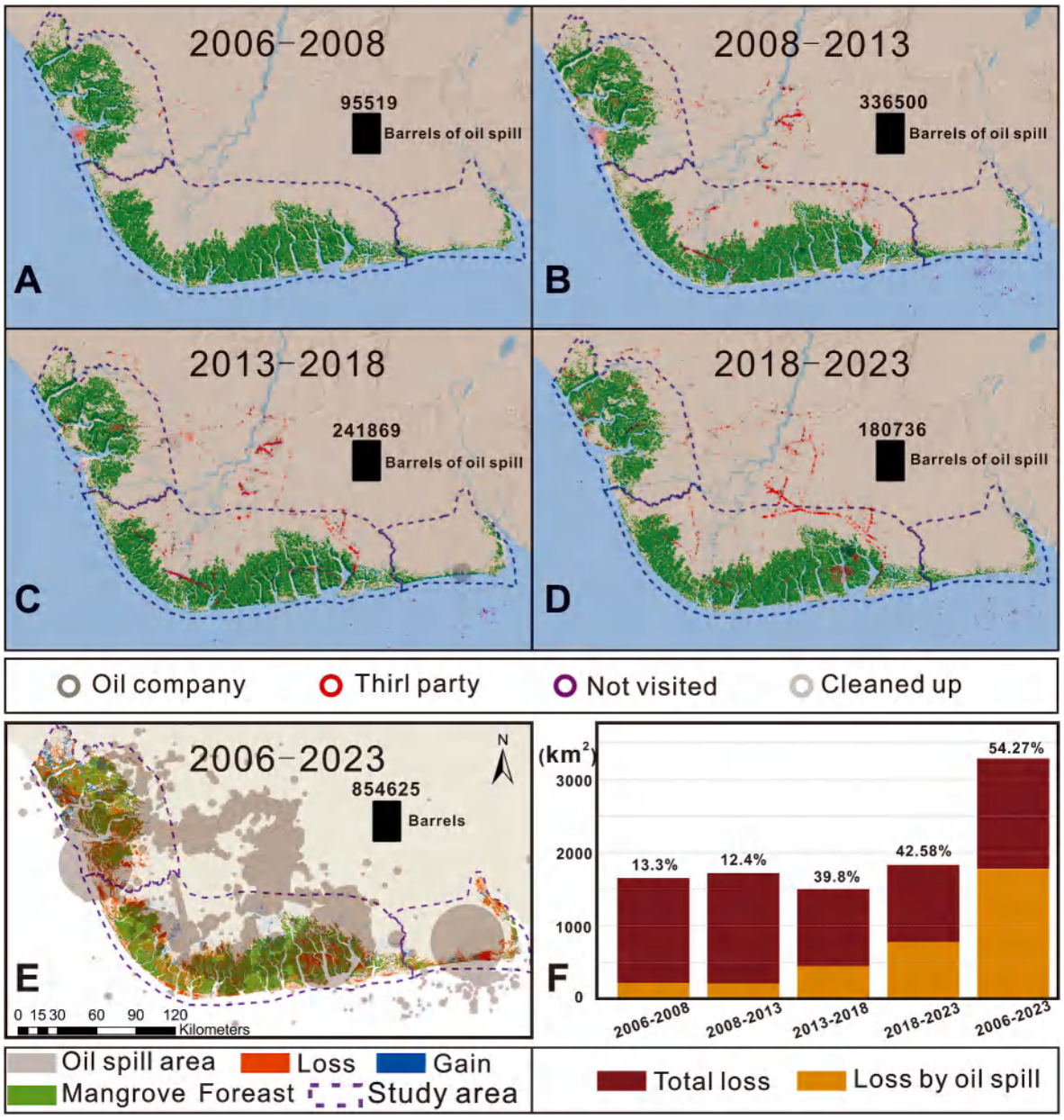

Fig. 8. Oil spills. (A–D) Interannual distribution of oil spills from 2006 to 2023, categorized by source and showing the oil spill volume in barrels for each period. (E) Combined map illustrating oil spill locations and the corresponding mangrove forest gain and loss areas during 2006–2023. (F) Percentage of total mangrove forests loss attributed to oil spills across different time intervals. (modified according to Nigerian Oil Spill Monitor, https://oilspillmonitor.ng/).

exists between urban expansion and mangrove coverage, with the significance level was below 0.05, demonstrating a strong correlation (Fig. 10C). This strong negative correlation suggests that as urban areas continue to expand, mangrove forest coverage consistently declines (Nababa, 2022). The dual pressures of oil spills and urban expansion underscore the detrimental impact of human activities on mangrove forest ecosystems. The frequent oil spills and rapid urbanization in the Niger Delta have collectively led to long-term environmental degradation and substantial mangrove forest loss (Zabbey et al., 2017).

4.4. Impacts of sea level rise

There is no doubt that sea-level rise caused by global warming has become a problem that cannot be ignored (Xu et al., 2022), and sea-level rise is also a widespread phenomenon in the Niger Delta, with an average rate of rise of 2.81 mm/yr (Daramola et al., 2022) (Fig. 11). As a result of significant sea level rise, mangrove forests in most parts of the world are being forced to migrate inland (Gilman et al., 2007; Liang, 2023; Mafi-Gholami et al., 2020). However, the vertical sedimentation rates, estimated based on the average beach slope, significantly exceed the rate of sea level rise: 72 mm/yr in the Eastern Niger Delta, 256 mm/yr in the Arcuate Niger Delta, and 90 mm/yr in the Western Niger Delta. Vertical sediment deposition rates significantly exceed sea level rise rates, so sea level rise could have a negligible effect on mangrove forests loss.

5. Conclusions

The mangrove forests in the Niger Delta hold significant importance as the largest mangrove forest in Africa. The dynamics of mangrove

Fig. 9. Consequences of oil spills in the Niger Delta. (A) Oil theft leading to environmental contamination, NOSDRA. (B) Oil spill cleanup efforts, NOSDRA. (C) Fire resulting from an oil spill, Nigerian Oil Spill Monitor. (D) Oil covering mangrove forests' roots, from Aa et al. (2022). (E, F) Vegetation loss caused by oil spills, from Onyena and Sam (2020). Nigerian Oil Spill Monitor and National Oil Spill Detection and Response Agency (NOSDRA) websites (https://oilspillmonitor.ng/, https://nosdra.gov.ng/).

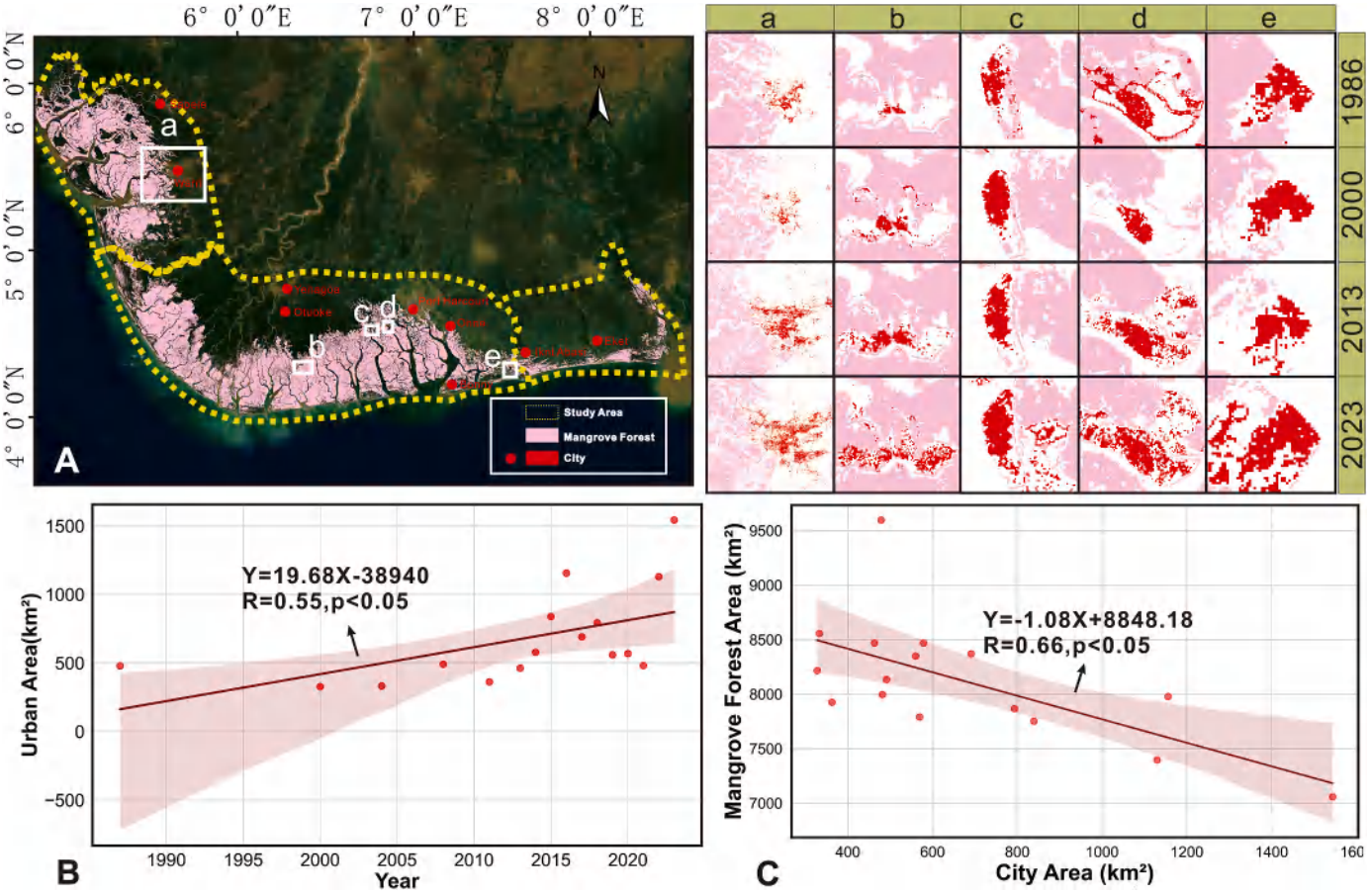

Fig. 10. The expansion of urban areas and its impact on mangrove forest habitats. (A) Spatio-temporal variation of urban areas and mangrove forests in the Niger Delta. (B) Temporal variation in the extent of urban areas in the Niger Delta from 1986 to 2023. (C) Correlation between urban area expansion and the decline in mangrove forest area.

forests in the Niger Delta exhibit considerable variations, and this study aims to provide a comprehensive assessment of the gain and loss of the Niger Delta's mangrove forests from 1988 to 2023. The major findings of the study are as follows.

(1) Throughout 1988–2023, the total area of the Niger Delta's mangrove forests decreased by 2536 km^2, leaving 7058 km2 by 2023. In addition, the regional trends differed markedly. Among

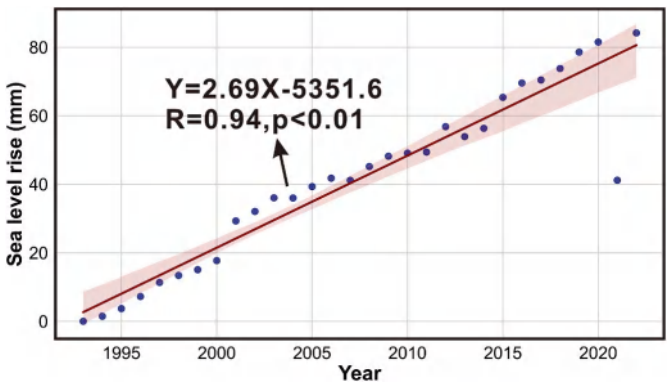

Fig. 11. The sea level rise and its simple linear regression analysis from 1993 to 2022 (https://cds.climate.copernicus.eu/cdsapp#!/home).

them, the East Niger Delta has the most dramatic decrease, with a decrease of nearly 58.7 %.

(2) The mangrove forests in the Niger Delta suffered from severe fragmentation, and the interior of the mangrove forests suffered from substantial loss. The edges of the mangrove forests moved landward at a rate of 13.58 m/yr. Notably, the seaward advance of the mangrove forest edges is observed in the estuary.

(3) Oil spills and urban sprawl occur as the primary causes for the significant degradation of the interior portions of mangrove forests, of which 54.27 % of the mangrove loss may have been caused by oil spills. Persistent erosion of mangrove forest edges may be affected by high-energy waves, and the difference in wave energy causes different degrees of erosion. By contrast, mangrove forest expansion in estuarine areas is due to increased river sediment supply.

These findings shed light on the changing dynamics and challenges faced by the mangrove forests in the Niger Delta. Oil spills, urban sprawl, and wave action have emerged as the primary drivers of mangrove forest degradation, and accelerating sea-level rise presents a growing threat to mangrove sustainability, while the increase in river sediment plays a crucial role in supporting the expansion and preservation of mangrove forests. Understanding these dynamics is vital for implementing effective conservation and management strategies to safeguard the resilience and ecological functions of the Niger Delta's mangrove forests.

CRediT authorship contribution statement

Diankai Wang: Writing – review & editing, Writing – original draft, Validation, Resources, Formal analysis. **Zhijun Dai:** Writing – review & editing, Writing – original draft, Visualization, Validation, Supervision, Software, Investigation, Formal analysis, Data curation, Conceptualization. **Chuqi Long:** Formal analysis, Data curation. **Xixing Liang:** Formal analysis, Data curation. **Yuan Xiong:** Formal analysis, Data curation, Conceptualization. **Jinping Cheng:** Writing – original draft, Investigation, Formal analysis, Data curation.

Declaration of competing interest

The authors declare that there is no conflicts of interest.

Acknowledgments

This research was supported by the National Natural Science Key Foundation of China (NSFC) (41930537), National Key R&D Program of China (2023YFE0121200), Shanghai International Science and Technology Cooperation Fund Project (23230713800), and International Joint Laboratory of Estuarine and Coastal Research, Shanghai (21230750600).

Data availability

Data will be made available on request.

References

Abam, T.K.S., 1999. Impact of dams on the hydrology of the Niger Delta. Bull. Eng. Geol. Environ. 57, 239–251. https://doi.org/10.1007/s100640050041.

Almar, R., Kestenare, E., Reyns, J., Jouanno, J., Anthony, E.J., Laibi, R., Hemer, M., Du Penhoat, Y., Ranasinghe, R., 2015. Response of the Bight of Benin (Gulf of Guinea, West Africa) coastline to anthropogenic and natural forcing, Part1: wave climate variability and impacts on the longshore sediment transport. Cont. Shelf Res. 110, 48–59. https://doi.org/10.1016/j.csr.2015.09.020.

Alongi, D., 2009. The energetics of mangrove forests. Energet. Mangr. Forests 1–216. https://doi.org/10.1007/978-1-4020-4271-3.

Ambrosini, D., Galli, G., Mancini, B., Nardi, I., Sfarra, S., 2014. Evaluating mitigation effects of urban heat Islands in a historical small center with the ENVI-Met® climate model. Sustainability 6, 7013–7029. https://doi.org/10.3390/su6107013.

Arifanti, V.B., Kauffman, J.B., Subarno, Ilman, M., Tosiani, A., Novita, N., 2022. Contributions of mangrove conservation and restoration to climate change mitigation in Indonesia. Glob. Change Biol. 28, 4523–4538. https://doi.org/10.1111/gcb.16216.

Balke, T., Bouma, T., Horstman, E., Webb, E., Erftemeijer, P., Herman, P., 2011. Windows of opportunity: thresholds to mangrove seedling establishment on tidal flats. Mar. Ecol. Prog. Ser. 440. https://doi.org/10.3354/meps09364.

Ball, MarilynC., 1988. Ecophysiology of mangroves. Trees (Berl.) 2. https://doi.org/10.1007/BF00196018.

Baloloy, A.B., Blanco, A.C., Sta Ana, R.R.C., Nadaoka, K., 2020. Development and application of a new mangrove vegetation index (MVI) for rapid and accurate mangrove mapping. Isprs J. Photogramm. Remote Sens. 166, 95–117. https://doi.org/10.1016/j.isprsjprs.2020.06.001.

Bennion, V., Hill, J.W., Lovelock, C.E., 2024. Mangrove surface elevation loss after tree fall during extreme weather. Wetlands 44, 113. https://doi.org/10.1007/s13157-024-01868-7.

Berger, U., Rivera-Monroy, V.H., Doyle, T.W., Dahdouh-Guebas, F., Duke, N.C., Fontalvo-Herazo, M.L., Hildenbrandt, H., Koedam, N., Mehlig, U., Piou, C., Twilley, R.R., 2008. Advances and limitations of individual-based models to analyze and predict dynamics of mangrove forests: a review. Aquat. Bot. 89, 260–274. https://doi.org/10.1016/j.aquabot.2007.12.015.

Breiman, L., 2001. Random forests. Mach. Learn. 45, 5–32. https://doi.org/10.1023/A:1010933404324.

Bryan, K.R., Nardin, W., Mullarney, J.C., Fagherazzi, S., 2017. The role of cross-shore tidal dynamics in controlling intertidal sediment exchange in mangroves in Cù Lao Dung, Vietnam. Cont. Shelf Res. 147, 128–143. https://doi.org/10.1016/j.csr.2017.06.014.

Cannon, D., Kibler, K., Donnelly, M., McClenachan, G., Walters, L., Roddenberry, A., Phagan, J., 2020. Hydrodynamic habitat thresholds for mangrove vegetation on the shorelines of a microtidal estuarine lagoon. Ecol. Eng. 158, 106070. https://doi.org/10.1016/j.ecoleng.2020.106070.

Carruthers, L., Ersek, V., Maher, D., Sanders, C., Tait, D., Soares, J., Floyd, M., Hashim, A. S., Helber, S., Garnett, M., East, H., Johnson, J.A., Ponta, G., Sippo, J.Z., 2024. Sea-level rise and extreme Indian Ocean dipole explain mangrove dieback in the Maldives. Sci. Rep. 14, 27012. https://doi.org/10.1038/s41598-024-73776-z.

Cazenave, A., Cozannet, G.L., 2014. Sea level rise and its coastal impacts. Earths Future 2, 15–34. https://doi.org/10.1002/2013EF000188.

Chang, D., Wang, Z., Ning, X., Li, Z., Zhang, L., Liu, X., 2022. Vegetation changes in Yellow River delta wetlands from 2018 to 2020 using PIE-engine and short time series sentinel-2 images. Front. Mar. Sci. 9, 977050. https://doi.org/10.3389/fmars.2022.977050.

Chen, D., Li, X., Saito, Y., Liu, J.P., Duan, Y., Liu, S., Zhang, L., 2020. Recent evolution of the irrawaddy (ayeyarwady) delta and the impacts of anthropogenic activities: a review and remote sensing survey. Geomorphology. https://doi.org/10.1016/j.geomorph.2020.107231.

Clough, B.F., 1992. Primary productivity and growth of mangrove forests. In: Tropical Mangrove Ecosystems. Coastal and Estuarine Studies, pp. 225–249. https://doi.org/10.1029/CE041p0225.

Comber, A., Fisher, P., Brunsdon, C., Khmag, A., 2012. Spatial analysis of remote sensing image classification accuracy. Remote Sens. Environ. 127, 237–246. https://doi.org/10.1016/j.rse.2012.09.005.

Dada, O.A., Li, G., Qiao, L., Asiwaju-Bello, Y.A., Anifowose, A.Y.B., 2018. Recent Niger Delta shoreline response to Niger River hydrology: conflict between forces of Nature and humans. J. Afr. Earth Sci. 139, 222–231. https://doi.org/10.1016/j.jafrearsci.2017.12.023.

Dada, O.A., Li, G., Qiao, L., Ma, Y., Ding, D., Xu, J., Li, P., Yang, J., 2016. Response of waves and coastline evolution to climate variability off the Niger Delta coast during the past 110years. J. Mar. Syst. 160, 64–80. https://doi.org/10.1016/j.jmarsys.2016.04.005.

Dada, O.A., Qiao, L., Ding, D., Li, G., Ma, Y., Wang, L., 2015. Evolutionary trends of the Niger Delta shoreline during the last 100years: responses to rainfall and river

discharge. Mar. Geol. 367, 202–211. https://doi.org/10.1016/j.margeo.2015.06.007.
Daramola, S., Li, H., Akinrinade, O., Hoenyedzi, G., Adenugba, O., 2022. Numerical assessment of potential sea level rise impacts on coastal retreat along the Nigerian Mahin mud coast. J. Coast Conserv. 26. https://doi.org/10.1007/s11852-022-00894-z.
Deng, Y., Jiang, W., Tang, Z., Ling, Z., Wu, Z., 2019. Long-term changes of open-surface water bodies in the Yangtze River basin based on the Google earth engine cloud platform. Remote Sens. https://doi.org/10.3390/rs11192213.
Dethier, E.N., Renshaw, C.E., Magilligan, F.J., 2022. Rapid changes to global river suspended sediment flux by humans. Science 376, 1447–1452. https://doi.org/10.1126/science.abn7980.
Dethier, E.N., Renshaw, C.E., Magilligan, F.J., 2020. Toward improved accuracy of remote sensing approaches for quantifying suspended sediment: implications for suspended-sediment monitoring. JGR Earth Surface 125, e2019JF005033. https://doi.org/10.1029/2019JF005033.
Dittmann, S., Mosley, L., Stangoulis, J., Nguyen, V.L., Beaumont, K., Dang, T., Guan, H., Gutierrez-Jurado, K., Lam-Gordillo, O., McGrath, A., 2022. Effects of extreme salinity stress on a temperate mangrove ecosystem. Front. For. Global Chang. 5–2022. https://doi.org/10.3389/ffgc.2022.859283.
Duke, N.C., Meynecke, J.-O., Dittmann, S., Ellison, A.M., Anger, K., Berger, U., Cannicci, S., Diele, K., Ewel, K.C., Field, C.D., Koedam, N., Lee, S.Y., Marchand, C., Nordhaus, I., Dahdouh-Guebas, F., 2007. A world without mangroves? Science 317, 41–42. https://doi.org/10.1126/science.317.5834.41b.
Eddy, S., Milantara, N., Sasmito, S.D., Kajita, T., Basyuni, M., 2021. Anthropogenic drivers of mangrove loss and associated carbon emissions in South Sumatra, Indonesia. Forests 12, 187. https://doi.org/10.3390/f12020187.
Effiong, S., Ubi, E., 2012. Oil Spillage Cost, Gas Flaring Cost and Life Expectancy Rate of the Niger Delta People of Nigeria, vol. 2, pp. 211–228.
Essien, J.P., Antai, S.P., 2009. Chromatium species: an emerging bioindicator of crude oil pollution of tidal mud flats in the Niger Delta mangrove ecosystem, Nigeria. Environ. Monit. Assess. 153, 95–102. https://doi.org/10.1007/s10661-008-0339-x.
Fan, C., Hou, X., Zhang, Y., Li, D., 2023. Satellite data reveal concerns regarding mangrove restoration efforts in southern China. Remote Sens. 15, 4151. https://doi.org/10.3390/rs15174151.
Farris, A.S., Long, J.W., Himmelstoss, E.A., 2023. Accuracy of shoreline forecasting using sparse data. Ocean Coast Manag. 239, 106621. https://doi.org/10.1016/j.ocecoaman.2023.106621.
Food and Agriculture Organization of the United Nations, 2007. In: The World's Mangroves, 1980-2005: a Thematic Study in the Framework of the Global Forest Resources Assessment 2005, FAO Forestry Paper. Food and Agriculture Organization of the United Nations, Rome.
Furukawa, K., Wolanski, E., 1996. Sedimentation in mangrove forests. Mangroves Salt Marshes 1, 3–10. https://doi.org/10.1023/A:1025973426404.
Furukawa, K., Wolanski, E., Mueller, H., 1997. Currents and sediment transport in mangrove forests. Estuar. Coast Shelf Sci. 44, 301–310. https://doi.org/10.1006/ecss.1996.0120.
Gao, B., 1996. NDWI—A normalized difference water index for remote sensing of vegetation liquid water from space. Remote Sens. Environ. 58, 257–266. https://doi.org/10.1016/S0034-4257(96)00067-3.
George, C.F., Macdonald, D.I.M., Spagnolo, M., 2019. Deltaic sedimentary environments in the Niger Delta, Nigeria. J. Afr. Earth Sci. 160, 103592. https://doi.org/10.1016/j.jafrearsci.2019.103592.
Ghosh, S.M., Behera, M.D., Paramanik, S., 2020. Canopy height estimation using sentinel series images through machine learning models in a mangrove Forest. Remote Sens. 12, 1519. https://doi.org/10.3390/rs12091519.
Gilman, E., Ellison, J., Coleman, R., 2007. Assessment of mangrove response to projected relative sea-level rise and recent historical reconstruction of shoreline position. Environ. Monit. Assess. https://doi.org/10.1007/s10661-006-9212-y.
Hagger, V., Worthington, T.A., Lovelock, C.E., Adame, M.F., Amano, T., Brown, B.M., Friess, D.A., Landis, E., Mumby, P.J., Morrison, T.H., O'Brien, K.R., Wilson, K.A., Zganjar, C., Saunders, M.I., 2022. Drivers of global mangrove loss and gain in social-ecological systems. Nat. Commun. 13, 6373. https://doi.org/10.1038/s41467-022-33962-x.
Hamilton, S.E., 2020. Botany of mangroves. In: Hamilton, S.E. (Ed.), Mangroves and Aquaculture: a Five Decade Remote Sensing Analysis of Ecuador's Estuarine Environments. Springer International Publishing, Cham, pp. 1–40. https://doi.org/10.1007/978-3-030-22240-6_1.
Heale, R., Twycross, A., 2015. Validity and reliability in quantitative studies. Evid. Base Nurs. 18, 66–67. https://doi.org/10.1136/eb-2015-102129.
Horstman, E.M., Dohmen-Janssen, C.M., Bouma, T.J., Hulscher, S.J.M.H., 2015. Tidal-scale flow routing and sedimentation in mangrove forests: combining field data and numerical modelling. Geomorphology 228, 244–262. https://doi.org/10.1016/j.geomorph.2014.08.011.
Hu, Z., Borsje, B.W., Van Belzen, J., Willemsen, P.W.J.M., Wang, H., Peng, Y., Yuan, L., De Dominicis, M., Wolf, J., Temmerman, S., Bouma, T.J., 2021. Mechanistic modeling of marsh seedling establishment provides a positive outlook for coastal wetland restoration under global climate change. Geophys. Res. Lett. 48, e2021GL095596. https://doi.org/10.1029/2021GL095596.
Hu, Z., Van Belzen, J., Van Der Wal, D., Balke, T., Wang, Z.B., Stive, M., Bouma, T.J., 2015. Windows of opportunity for salt marsh vegetation establishment on bare tidal flats: the importance of temporal and spatial variability in hydrodynamic forcing. J. Geophys. Res.: Biogeosciences 120, 1450–1469. https://doi.org/10.1002/2014JG002870.
Iwegbue, C.M.A., Bebenimibo, E., Obi, G., Tesi, G.O., Olisah, C., Egobueze, F.E., Martincigh, B.S., 2021. Distribution and sources of n-Alkanes and polycyclic aromatic hydrocarbons in sediments around oil production facilities in the Escravos River Basin, Niger Delta, Nigeria. Arch. Environ. Contam. Toxicol. 80, 474–489. https://doi.org/10.1007/s00244-021-00810-w.
Izah, S.C., 2018. Ecosystem of the Niger Delta region of Nigeria: potentials and threats. Biodiver. Int. J. 2, 338–345. https://doi.org/10.15406/bij.2018.02.00084.
Jaman, F., 2023. The effect of oil spill on the sundarban mangrove forest of Bangladesh. Central Asian Stud. 4.
James, G.K., Adegoke, J.O., Saba, E., Nwilo, P., Akinyede, J., 2007a. Satellite-based assessment of the extent and changes in the mangrove ecosystem of the Niger Delta. Mar. Geod. 30, 249–267. https://doi.org/10.1080/01490410701438224.
James, G.K., Adegoke, J.O., Saba, E., Nwilo, P., Akinyede, J., 2007b. Satellite-Based assessment of the extent and changes in the mangrove ecosystem of the Niger Delta. Mar. Geod. 30, 249–267. https://doi.org/10.1080/01490410701438224.
Jia, M., Wang, Z., Mao, D., Ren, C., Song, K., Zhao, C., Wang, C., Xiao, X., Wang, Y., 2023. Mapping global distribution of mangrove forests at 10-m resolution. Sci. Bull. 68, 1306–1316. https://doi.org/10.1016/j.scib.2023.05.004.
John, R.C., Okpokwasili, G.C., 2012. Crude oil-degradation and plasmid profile of nitrifying bacteria isolated from oil-impacted mangrove sediment in the Niger Delta of Nigeria. Bull. Environ. Contam. Toxicol. 88, 1020–1026. https://doi.org/10.1007/s00128-012-0609-8.
Kuta, A.A., Grebby, S., Boyd, D.S., 2025. Remote monitoring of the impact of oil spills on vegetation in the Niger Delta, Nigeria. Appl. Sci. 15, 338. https://doi.org/10.3390/app15010338.
Lassalle, G., Scafutto, R.D.M., Lourenço, R.A., Mazzafera, P., De Souza Filho, C.R., 2023. Remote sensing reveals unprecedented sublethal impacts of a 40-year-old oil spill on mangroves. Environ. Pollut. 331, 121859. https://doi.org/10.1016/j.envpol.2023.121859.
Lee, S.Y., Primavera, J.H., Dahdouh-Guebas, F., McKee, K., Bosire, J.O., Cannicci, S., Diele, K., Fromard, F., Koedam, N., Marchand, C., Mendelssohn, I., Mukherjee, N., Record, S., 2014. Ecological role and services of tropical mangrove ecosystems: a reassessment. Global Ecol. Biogeogr. 23, 726–743. https://doi.org/10.1111/geb.12155.
Liang, S., 2023. Mapping mangrove sustainability in the face of sea level rise and land use: a case study on leizhou peninsula, China. J. Environ. Manag. 325, 116554. https://doi.org/10.1016/j.jenvman.2022.116554.
Linden, O., Palsson, J., 2013. Oil contamination in Ogoniland, Niger Delta. Ambio 42, 685–701. https://doi.org/10.1007/s13280-013-0412-8.
Ling, Z., Jiang, W., Peng, K., Zhang, Z., Wu, Z., Zhong, S., Chu, A., Xiao, Z., Sun, Z., 2024. SDG- and GMAG-oriented analysis of multi scenarios spatiotemporal changes and evaluation of the effectiveness and potential of mangrove forests. Int. J. Dig. Earth 17, 2346274. https://doi.org/10.1080/17538947.2024.2346274.
Liu, X., Liu, J.P., Wang, Y.P., 2023. Editorial: sediment dynamics and geohazards in estuaries and deltas. Front. Earth Sci. 10, 1079804. https://doi.org/10.3389/feart.2022.1079804.
Long, C., Dai, Z., Zhou, X., Mei, X., Mai, Van C., 2021. Mapping mangrove forests in the Red River Delta, Vietnam. For. Ecol. Manag. 483, 118910. https://doi.org/10.1016/j.foreco.2020.118910.
Lotfinasabasl, S., Gunale, V.R., Rajurkar, N.S., 2013. Petroleum hydrocarbons pollution in soil and its bioaccumulation in mangrove species, Avicennia marina from Alibaug mangrove ecosystem. Maharashtra, India 2.
Lovelock, C.E., Cahoon, D.R., Friess, D.A., Guntenspergen, G.R., Krauss, K.W., Reef, R., Rogers, K., Saunders, M.L., Sidik, F., Swales, A., Saintilan, N., Thuyen, L.X., Triet, T., 2015. The vulnerability of indo-pacific mangrove forests to sea-level rise. Nature 526, 559–563. https://doi.org/10.1038/nature15538.
MacKenzie, R.A., Foulk, P.B., Klump, J.V., Weckerly, K., Purbospito, J., Murdiyarso, D., Donato, D.C., Nam, V.N., 2016. Sedimentation and belowground carbon accumulation rates in mangrove forests that differ in diversity and land use: a tale of two mangroves. Wetl. Ecol. Manag. 24, 245–261. https://doi.org/10.1007/s11273-016-9481-3.
Mafi-Gholami, D., Zenner, E.K., Jaafari, A., 2020. Mangrove regional feedback to sea level rise and drought intensity at the end of the 21st century. Ecological Indicators 110, 105972. https://doi.org/10.1016/j.ecolind.2019.105972.
Montero, D., Aybar, C., Mahecha, M.D., Martinuzzi, F., Söchting, M., Wieneke, S., 2023. A standardized catalogue of spectral indices to advance the use of remote sensing in Earth system research. Sci. Data 10, 197. https://doi.org/10.1038/s41597-023-02096-0.
Moschetto, F.A., Ribeiro, R.B., De Freitas, D.M., 2021. Urban expansion, regeneration and socioenvironmental vulnerability in a mangrove ecosystem at the southeast coastal of são paulo, Brazil. Ocean Coast Manag. 200, 105418. https://doi.org/10.1016/j.ocecoaman.2020.105418.
Mosquera, E., Blanco-Libreros, J.F., Riascos, J.M., 2023. Are urban mangroves emerging hotspots of non-indigenous species? A study on the dynamics of macrobenthic fouling communities in fringing red mangrove prop roots. Biol. Invasions 25, 787–800. https://doi.org/10.1007/s10530-022-02944-x.
Nababa, I., Symeonakis, E., Koukoulas, S., Higginbottom, T., Cavan, G., Marsden, S., 2020. Land cover dynamics and mangrove degradation in the Niger Delta Region. Remote Sens. 12, 3619. https://doi.org/10.3390/rs12213619.
Nababa, I.I., 2022. Monitoring and Modelling Disturbances to the Niger Delta Mangrove Forests (Phd Thesis). Manchester Metropolitan University.
Nababa, I.I., Symeonakis, E., Koukoulas, S., Higginbottom, T.P., Cavan, G., Marsden, S., 2020. Land cover dynamics and mangrove degradation in the Niger Delta region. Remote Sens. 12. https://doi.org/10.3390/rs12213619.
Nassar, K., Mahmod, W.E., Fath, H., Masria, A., Nadaoka, K., Negm, A., 2019. Shoreline change detection using DSAS technique: case of North Sinai coast, Egypt. Mar. Georesour. Geotec. 37, 81–95. https://doi.org/10.1080/1064119X.2018.1448912.

Numbere, A.O., 2018. The impact of oil and gas exploration: invasive nypa palm species and urbanization on mangroves in the Niger River Delta, Nigeria. In: Makowski, C., Finkl, C. (Eds.), Threats to Mangrove Forests: Hazards, Vulnerability. and Management, pp. 247–266. https://doi.org/10.1007/978-3-319-73016-5_12.

Nwankwo, D.I., 2000. The algae of crude oil impacted mangrove soil in the Niger Delta, Nigeria. Trop. Ecol. 41, 243–245.

Nwobi, C., Williams, M., Mitchard, E.T.A., 2020. Rapid mangrove Forest loss and nipa palm (Nypa fruticans) expansion in the Niger Delta, 2007–2017. Remote Sens. 12, 2344. https://doi.org/10.3390/rs12142344.

O'Farrell, J., O'Fionnagáin, D., Babatunde, A.O., Geever, M., Codyre, P., Murphy, P.C., Spillane, C., Golden, A., 2025. Quantifying the impact of crude oil spills on the mangrove ecosystem in the Niger Delta using AI and Earth observation. Remote Sens. 17, 358. https://doi.org/10.3390/rs17030358.

Onyena, A.P., Sam, K., 2020. A review of the threat of oil exploitation to mangrove ecosystem: insights from Niger Delta, Nigeria. Global Ecol. Conserv. 22, e00961. https://doi.org/10.1016/j.gecco.2020.e00961.

Pham, L.T.H., Brabyn, L., 2017. Monitoring mangrove biomass change in Vietnam using SPOT images and an object-based approach combined with machine learning algorithms. Isprs J. Photogramm. Remote Sens. 128, 86–97. https://doi.org/10.1016/j.isprsjprs.2017.03.013.

Pilato, C., 2019. Hydrodynamic Limitations and the Effects of Living Shoreline Stabilization on Mangrove Recruitment Along Florida Coastlines. University of Central Florida.

Raji, A.O.Y., Abejide, T.S., 2013. An assessment of environmental problems associated with oil pollution and gas flaring in the Niger Delta Region Nigeria , C. 1960s - 2000. Oman Chapt. Arab. J. Bus. Manag. Rev. 3, 48–62. https://doi.org/10.12816/0016430.

Sahana, M., Areendran, G., Sajjad, H., 2022. Assessment of suitable habitat of mangrove species for prioritizing restoration in coastal ecosystem of Sundarban Biosphere Reserve, India. Sci. Rep. 12, 20997. https://doi.org/10.1038/s41598-022-24953-5.

Sánchez-Núñez, D.A., Bernal, G., Mancera Pineda, J.E., 2019a. The relative role of mangroves on wave erosion mitigation and sediment properties. Estuaries Coasts 42, 2124–2138. https://doi.org/10.1007/s12237-019-00628-9.

Sánchez-Núñez, D.A., Bernal, G., Mancera Pineda, J.E., 2019b. The relative role of mangroves on wave erosion mitigation and sediment properties. Estuaries Coasts 42, 2124–2138. https://doi.org/10.1007/s12237-019-00628-9.

Santos, A.A., Santos, D.M.C., Lira, C.F., 2024. Keys to successful restoration of a mangrove Forest after an oil spill accident: a case study in Brazil. https://doi.org/10.2139/ssrn.4808268.

Saunders, D., Carrillo, J.C., Gundlach, E.R., Iroakasi, O., Visigah, K., Zabbey, N., Bonte, M., 2022. Analysis of polycyclic aromatic hydrocarbons (PAHs) in surface sediments and edible aquatic species in an oil-contaminated mangrove ecosystem in Bodo, Niger Delta, Nigeria: bioaccumulation and human health risk assessment. Sci. Total Environ. 832. https://doi.org/10.1016/j.scitotenv.2022.154802.

Sexton, W.J., Murday, M., 1994. The morphology and sediment character of the coastline of Nigeria-the Niger Delta. J. Coast Res. 10, 959–977.

Shirmohammadi, M., Mafi-Gholami, D., Pirasteh, S., Youssefi, F., Shen, J., Li, W., Li, J., 2024. Assessing climatic change impacts on mangrove structural dynamics on the northern coasts of the Persian Gulf. ISPRS Ann. Photogramm. Remote Sens. Spatial Inf. Sci. X-3 (2024), 383–386. https://doi.org/10.5194/isprs-annals-X-3-2024-383-2024.

Shwetakshi, M., 2023. Impact of urbanization on declining mangrove health of Goa. Int. J. Res. Publ. Rev. 4, 1566–1574. https://doi.org/10.55248/gengpi.2023.4144.

Stiepani, J., Gillis, L.G., Chee, S.Y., Pfeiffer, M., Nordhaus, I., 2021. Impacts of urbanization on mangrove forests and brachyuran crabs in Penang, Malaysia. Reg. Environ. Change 21, 69. https://doi.org/10.1007/s10113-021-01800-3.

Stutz, M.L., Pilkey, O.H., 2002. Global distribution and morphology of deltaic barrier island systems. J. Coast Res. 694–707. https://doi.org/10.2112/1551-5036-36.sp1.694.

Teluguntla, P., Thenkabail, P.S., Oliphant, A., Xiong, J., Gumma, M.K., Congalton, R.G., Yadav, K., Huete, A., 2018. A 30-m landsat-derived cropland extent product of Australia and China using random forest machine learning algorithm on Google Earth engine cloud computing platform. Isprs J. Photogramm. Remote Sens. 144, 325–340. https://doi.org/10.1016/j.isprsjprs.2018.07.017.

Thampanya, U., Vermaat, J.E., Sinsakul, S., Panapitukkul, N., 2006. Coastal erosion and mangrove progradation of Southern Thailand. Estuarine. Coast. Shelf Sci. 68, 75–85. https://doi.org/10.1016/j.ecss.2006.01.011.

Thomas, N., Lucas, R., Bunting, P., Hardy, A., Rosenqvist, A., Simard, M., 2017. Distribution and drivers of global mangrove forest change, 1996–2010. PLoS One 12, e0179302. https://doi.org/10.1371/journal.pone.0179302.

Tomlinson, P.B., 2016. The Botany of Mangroves, second ed. Cambridge University Press, Cambridge. https://doi.org/10.1017/CBO9781139946575.

Tuholske, C., Halpern, B.S., Blasco, G., Villasenor, J.C., Frazier, M., Caylor, K., 2021. Mapping global inputs and impacts from of human sewage in coastal ecosystems. PLoS One 16, e0258898. https://doi.org/10.1371/journal.pone.0258898.

Tuholske, C., Tane, Z., López-Carr, D., Roberts, D., Cassels, S., 2017. Thirty years of land use/cover change in the Caribbean: assessing the relationship between urbanization and mangrove loss in Roatán, Honduras. Appl. Geogr. 88, 84–93. https://doi.org/10.1016/j.apgeog.2017.08.018.

Van Santen, P., Augustinus, P.G.E.F., Janssen-Stelder, B.M., Quartel, S., Tri, N.H., 2007. Sedimentation in an estuarine mangrove system. J. Asian Earth Sci. 29, 566–575. https://doi.org/10.1016/j.jseaes.2006.05.011.

Veettil, B.K., Ward, R.D., Quang, N.X., Trang, N.T.T., Giang, T.H., 2019. Mangroves of Vietnam: historical development, current state of research and future threats. Estuar. Coast Shelf Sci. 218, 212–236. https://doi.org/10.1016/j.ecss.2018.12.021.

Vo Luong, P., Massel, S., 2006. Experiments on wave motion and suspended sediment concentration at Nang Hai, can Gio mangrove forest, Southern Vietnam. Oceanologia 48.

Wang, D., Wan, B., Qiu, P., Su, Y., Guo, Q., Wu, X., 2018. Artificial mangrove species mapping using Pléiades-1: an evaluation of pixel-based and object-based classifications with selected machine learning algorithms. Remote Sens. 10, 294. https://doi.org/10.3390/rs10020294.

Wang, F., Shu-ming, L., Wen-hu, L., Qiong-wei, D., Wei-nan, J., Jin, L., 2014. Island instantaneous coastline extraction based on the characteristics of regional statistics of multispectral remote sensing image. Mar. Sci. Bull.

Wang, H., Peng, Y., Wang, C., Wen, Q., Xu, J., Hu, Z., Jia, X., Zhao, X., Lian, W., Temmerman, S., Wolf, J., Bouma, T., 2021. Mangrove loss and gain in a densely populated urban Estuary: lessons from the Guangdong-Hong Kong-Macao greater Bay area. Front. Mar. Sci. 8, 693450. https://doi.org/10.3389/fmars.2021.693450.

Wang, M., Mao, D., Wang, Y., Song, K., Yan, H., Jia, M., Wang, Z., 2022. Annual wetland mapping in metropolis by temporal sample migration and random forest classification with time series landsat data and google Earth engine. Remote Sens. 14, 3191. https://doi.org/10.3390/rs14133191.

Wanzhen, X., Majid, N.A., 2024. The association between rapid urbanization process and mangrove land use changes in coastal regions of mainland China: a ten-years systematic review. Rev. Gestão Soc. e Ambiental 18, e05476. https://doi.org/10.24857/rgsa.v18n2-125.

Wardlow, B.D., Egbert, S.L., Kastens, J.H., 2007. Analysis of time-series MODIS 250 m vegetation index data for crop classification in the U.S. Central Great Plains. Remote Sens. Environ. 108, 290–310. https://doi.org/10.1016/j.rse.2006.11.021.

Williams, L.J., Cavender-Bares, J., Townsend, P.A., Couture, J.J., Wang, Z., Stefanski, A., Messier, C., Reich, P.B., 2020. Remote spectral detection of biodiversity effects on forest biomass. Nat. Ecol. Evolut. 5, 46–54. https://doi.org/10.1038/s41559-020-01329-4.

Wolanski, E., Williams, D., Hanert, E., 2006. The sediment trapping efficiency of the macro-tidal Daly Estuary, tropical Australia. Estuar. Coast Shelf Sci. 69, 291–298. https://doi.org/10.1016/j.ecss.2006.04.023.

Woodroffe, C.D., Rogers, K., McKee, K.L., Lovelock, C.E., Mendelssohn, I.A., Saintilan, N., 2016a. Mangrove sedimentation and response to relative sea-level rise. Ann. Rev. Mar. Sci 8, 243–266. https://doi.org/10.1146/annurev-marine-122414-034025.

Woodroffe, C.D., Rogers, K., McKee, K.L., Lovelock, C.E., Mendelssohn, I.A., Saintilan, N., 2016b. Mangrove sedimentation and response to relative sea-level rise. Ann. Rev. Mar. Sci 8, 243–266. https://doi.org/10.1146/annurev-marine-122414-034025.

Wu, S., Yuan, B., Liu, S., Wang, Q., Liu, J., Yan, C., Hong, H., Pavao-Zuckerman, M.A., Lu, H., 2024. Urbanization-driven anthropogenic and environmental factors shape soil dissolved organic matter in mangrove ecosystems. Ecosys. Health Sustain. 10, 154. https://doi.org/10.34133/ehs.0154.

Xiao, Z., Jiang, W., Wu, Z., Ling, Z., Deng, Y., Zhang, Z., Peng, K., 2024. Agreement analysis and accuracy assessment of multiple mangrove datasets in guangxi beibu gulf and guangdong-hong kong-macau greater bay, China, for 2000–2020. IEEE J. Sel. Top. Appl. Earth Obs. Rem. Sens. 17, 3438–3451. https://doi.org/10.1109/JSTARS.2024.3353251.

Xiong, Y., Dai, Z., Long, C., Liang, X., Lou, Y., Mei, X., Nguyen, B.A., Cheng, J., 2024. Machine learning-based examination of recent mangrove forest changes in the Western Irrawaddy River Delta, southeast asia. Catena 234, 107601. https://doi.org/10.1016/j.catena.2023.107601.

Xu, H., Hou, X., Li, D., Wang, X., Fan, C., Du, P., Song, B., 2022. Spatial assessment of coastal flood risk due to sea level rise in China's coastal zone through the 21st century. Front. Mar. Sci. 9, 945901. https://doi.org/10.3389/fmars.2022.945901.

Yao, J., Wu, J., Xiao, C., Zhang, Z., Li, J., 2022. The classification method Study of crops remote sensing with deep learning, machine learning, and Google Earth engine. Remote Sens. 14, 2758. https://doi.org/10.3390/rs14122758.

Zabbey, N., Sam, K., Onyebuchi, A.T., 2017. Remediation of contaminated lands in the Niger Delta, Nigeria: prospects and challenges. Sci. Total Environ. 586, 952–965. https://doi.org/10.1016/j.scitotenv.2017.02.075.

Zhang, L., Hu, Q., Tang, Z., 2022. Assessing the contemporary status of Nebraska's eastern saline wetlands by using a machine learning algorithm on the Google Earth Engine cloud computing platform. Environ. Monit. Assess. 194, 193. https://doi.org/10.1007/s10661-022-09850-8.